



HAL
open science

Effect of Precious Metals on NO Reduction by CO in Oxidative Conditions

Joudia Akil, Stéphane Siffert, Laurence Pirault-Roy, Damien Debecker, François Devred, Renaud Cousin, Christophe Poupin

► **To cite this version:**

Joudia Akil, Stéphane Siffert, Laurence Pirault-Roy, Damien Debecker, François Devred, et al.. Effect of Precious Metals on NO Reduction by CO in Oxidative Conditions. Applied Sciences, 2020, 10 (9), pp.3042. 10.3390/app10093042 . hal-03533601

HAL Id: hal-03533601

<https://hal.science/hal-03533601>

Submitted on 20 Mar 2023

HAL is a multi-disciplinary open access archive for the deposit and dissemination of scientific research documents, whether they are published or not. The documents may come from teaching and research institutions in France or abroad, or from public or private research centers.

L'archive ouverte pluridisciplinaire **HAL**, est destinée au dépôt et à la diffusion de documents scientifiques de niveau recherche, publiés ou non, émanant des établissements d'enseignement et de recherche français ou étrangers, des laboratoires publics ou privés.

Effect of precious metals on NO reduction by CO in oxidative conditions

Joudia Akil¹, Stéphane Siffert^{1*}, Laurence Pirault-Roy², Damien P. Debecker³, François Devred³, Renaud Cousin¹, Christophe Poupin^{1*}

¹ Univ. Littoral Côte d'Opale, UR 4492, UCEIV, Unité de Chimie Environnementale et Interactions sur le Vivant, 149 Avenue Maurice Schumann, 59140 Dunkerque, France

² Institute of Chemistry of Poitiers: materials and natural resources (IC2MP) UMR-CNRS 7285, University of Poitiers, 4, rue Michel Brunet (Bât B27) 86073 Poitiers Cedex, France

³ Institute of Condensed Matter and Nanoscience (IMCN), Université Catholique de Louvain, Place Louis Pasteur, 1, Box L4.01.09, 1348 Louvain la-Neuve, Belgium

* Correspondence: poupin@univ-littoral.fr (C.); siffert@univ-littoral.fr (S.); Tel.: +33-328237691 (C.) ; +33-328658256 (S.)

Abstract: Carbon dioxide has become an environmental challenge, where the emissions have reached higher level than what could be handled. In this regard, conversion of CO₂ to value-added chemicals and thus recycling CO₂ appeared a viable option. Prior to valorization, CO₂ must be purified. Among several opportunities, oxyfuel combustion is a process in strong development. However, the gases resulting from this process contain some traces of impurities that can hinder the recovery of CO₂ such as NO and CO. This work has therefore focused on the study of the reaction of NO-CO reaction in an oxidizing medium, using heterogeneous catalytic materials based on various supported noble metals. These materials were extensively characterized by a variety of methods including BET surface area measurements, hydrogen chemisorption, Transmission Electron Microscopy (TEM) and H₂ temperature programmed reduction (H₂-TPR). The obtained results show that the catalytic behavior of M/Al₂O₃ catalysts in CO oxidation and NO reduction with CO in oxidative conditions depends mainly on the nature of the metal. The best result for both reactions is obtained with Pt/Al₂O₃ catalyst. The Pt nanoparticles in their metallic form (Pt⁰) as evidenced by TPR could explain the activity.

Keywords: Environmental chemistry; Oxyfuel Combustion; NO-CO reaction; Heterogeneous catalysis.

1. Introduction

Greenhouse gases (GHG) emissions generated by human activity led to an increase in the radiation which is trapped in the atmosphere and induced an increase in the greenhouse effect. This is mainly due to carbon dioxide (CO₂), representing 79% of GHG [1]. The CO₂ emitted from anthropic activities, is perceived as a constraint in industrial activity with taxes, stringent environmental regulations, impact on global warming... To limit these CO₂ emissions, it could be considered as a gas with industrial advantage and/or as a new source of carbon for the production of minerals or organic compounds with commercial interest. Reuse of CO₂ represents a promising alternative, with important applications in chemical industry and for power generation.

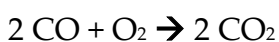
The processes for the valorization of CO₂ can be divided into three different categories:[2]

- Direct use without transformation: industrial use (water treatment, supercritical CO₂ ...).
- Chemical transformation: organic chemical synthesis, methanation, hydrogenation (methanol), reforming: dry (CO₂) or steam reforming (CO₂ + H₂O)...
- Biological transformation: microalgae, biocatalysis.

However, CO₂ valorization process requires a gas as pure as possible [2].

Oxyfuel-combustion is therefore a promising method to get a nearly pure CO₂ that enables to obtain a CO₂ rich stream (80%) [3]. In the oxyfuel system, the combustion flow consists of pure O₂ obtained by air distillation. By excluding dinitrogen from oxidizing flow, the production of NO_x is limited as well as the amount of smoke generated. This NO_x emission limitation is interesting as NO_x are considered as one of the main pollutants of the atmosphere, since they are responsible for a lot of environmental problems like photochemical smog, acid rains, ozone layer depletion [4]. This process emits also water vapor, unburned components (in function of the waste burned) such as carbon monoxide (generated by incomplete combustion) in addition to nitrogen monoxide [3]. CO is the cheapest and the most available compound from industrial sources and it could be used as a reductant of NO although it is known to be one of the worst reductants. P. Malfoy ranked, several reducers according the NO half-conversion temperatures achieved using noble metals. The sequence obtained is as follows: H₂ > NH₃ > CO > C₃H₅ [5]. So it seems possible to purify the CO₂ issued from oxyfuel-combustion by NO-CO reaction which consists of the main challenge that our work tried to lift up.

In oxyfuel combustion systems, NO, CO, O₂ are simultaneously present and the following reactions may occur [6]:



Therefore as oxygen is present in excess, it competes with NO for oxidizing the reducing agent (CO) [7]. Due to this effect, many authors studied the competitions between CO-NO and CO-O₂ reactions. Shelef et al. demonstrated that the second reaction is predominant over a number of transition metal oxides and supported Pt [8]. Other authors proved that the NO addition to CO+O₂ mixture reduces drastically the rate of CO₂ formation on Rh catalyst [9] and Pt supported catalyst [10].

The NO–CO reaction has been widely applied and investigated over various catalysts. For example, three-way catalysts (TWC), composed of noble metals (Rh, Pd and Pt), convert CO, NO, and hydrocarbons simultaneously [11]. Rh is employed for NO removal because it combines a good activity and selectivity to form nitrogen [12]. On the other hand, Pt and Pd ensure the oxidation of CO and hydrocarbons [13]. Kobylinski and Taylor [14] studied NO reduction over supported Pt, Rh, Pd and Ru. They proved that, when CO is used as reducing agent, the reaction over Ru catalyst is accelerated. The activity sequence of the catalysts was: Ru > Rh > Pt > Pd. It was also studied for this reaction in presence of O₂ [7,15]. It has been demonstrated that Ir effectively promotes the NO-CO reaction in the presence of an excess of oxygen.

To summarize, the objective is to reduce NO by CO in an oxidizing environment with a CO₂ rich stream in order to purify the latest without the use of a SCR system (Selective Catalytic Reduction) that would switch to a reductive atmosphere by injecting additives (ammonia or urea)[11]. The important amount of CO₂ could be a problem for materials with basic properties due to carbonate species formation. Alumina was then chosen because of its strong Lewis acid centers which ensure the stabilization of species in active state and disperses them adequately, as well as its intrinsic catalytic activity in various reactions [13,16]. This paper will present you the results obtained by using different precious metals (Pt, Pd, Rh, Ru and Ir) catalysts supported on alumina tested for NO-CO reaction.

2. Materials and Methods

2.1. Catalysts preparation

Alumina (Degussa Aluminum Oxid C) with a specific surface area of 100 m².g⁻¹ was used as support. After calcination of support for 4 h at 500 °C under air, the catalysts were prepared by wet impregnation of alumina with corresponding nitrous or acetylacetonate (acac) precursors as indicated in the following table (table 1). For all catalysts, the nominal metallic content was of 1.0 wt%.

Table 1. Metal precursors

Metal precursor used	Iridium	Palladium	Platinum	Rhodium	Ruthenium
	Ir(acac) ₃	Pd(acac) ₂	Pt(NO ₂) ₂ (NO ₃) ₂	Rh(NO ₃) ₃	Ru(acac) ₃

The slurry was shaken at room temperature for 12 h and after drying in a sand bath at 80 °C, the impregnated alumina was left overnight in an oven at 120 °C. Then, the sample was calcined in dry air (4 h, 500 °C) and reduced under pure H₂ flow (2 h, 500°C).

2.2. Characterization of the catalysts

Before any impregnation, the support used (Al₂O₃) was characterized by nitrogen physisorption. The surface area was determined from N₂ adsorption/desorption isotherms measured at -196 °C with BET surface analyzer (Micromeritics Model TRISTAR 3000) using Brunauer-Emmett-Teller (BET) and the pore size distribution based on Baret–Joyner–Halenda (BJH) methods). Before the analysis, the samples were outgassed at 250 °C under vacuum overnight.

The H₂ chemisorption capacity was determined by a static volumetric vacuum technique at room temperature, except for Pd catalyst for which the experiment was run at 70°C in order to avoid palladium hydrides formation. Firstly, the catalyst was cleaned under ultra-high vacuum overnight to eliminate the adsorbed molecules. Then, the catalyst was reduced under 750 mbar of H₂ for 1 h at 300 °C, and purged under vacuum until reaching a low pressure ($P < 10^{-5}$ mbar). Two series of hydrogen adsorption isotherms were performed with an increasing hydrogen pressure, from 10 to 70 mbar in steps of 10 mbar. Between the two series, the sample was submitted to ultrahigh vacuum in order to remove weakly bound hydrogen. The adsorbed hydrogen quantity was calculated by extrapolating the isotherm to $P = 0$. The first isotherm allows determining the total amount of adsorbed hydrogen and the second one the amount of physisorbed hydrogen. The chemisorbed hydrogen amount was calculated by difference between these two values for Ir/Al₂O₃ and Pt/Al₂O₃. Concerning the Rh/Al₂O₃ and Pd/Al₂O₃, only the first isotherm is used to determinate the amount of adsorbed hydrogen due to a very low H₂ physisorption on these materials. The metal particle size was calculated considering a stoichiometry of H/M = 1, and assuming that particles correspond to cubes deposited on the support and exposing 5 faces [17], with an equal distribution between (1 1 1), (1 1 0) and (1 0 0) planes.

In order to consolidate the results obtained with hydrogen chemisorption, transmission electron microscopy (TEM) analysis was performed with a JEOL 2100 electron microscope operating at 200 kV with a theoretical resolution of 0.19 nm. Catalysts were finely ground, dispersed in ethanol using an ultrasonic bath and finally deposited on the carbon film of a copper grid. The particle size distribution was estimated on the basis of TEM pictures analysis using ImageJ software and the average particle diameter was determined from the measurement performed on at minimum 100 particles.

H₂ temperature programmed reductions (TPR) were performed on a Hiden Catlab equipped with QGA Hiden quadrupole mass spectrometer. The catalysts were first pretreated at 200°C for 1 hour under argon (20 mL/min Air Liquide 5.0).

The sample was then cooled down to 80°C and exposed to a mixture of 0.25 % H₂ in inert atmosphere. The TPR was then carried out using a ramp of 10 °C.min⁻¹ up to 500 °C.

2.3. Catalytic tests

Before each test, the catalyst was treated in situ under He flow (40 mL.min⁻¹) at 200 °C for 1.5 h. Then, CO₂ purification was carried out at atmospheric pressure in a fixed-bed flow reactor containing 150 mg of catalyst. The catalysts were sieved in order to retain grains with diameters between 0.315 and 0.500 mm and diluted to a constant volume by SiC (exhibited no activity in CO₂ purification from 50 to 500 °C) so that all the experiments were carried out under the same conditions (GHSV = 2.24 10⁴ h⁻¹).

The flow of the reactant gases is composed of: 20 % CO₂, 10 % O₂, 0.5 % CO and 0.02 % NO (He as eluent gas) with a total flow of 200 mL.min⁻¹, in the temperature range 50–500 °C. The reaction products (CO₂ and N₂) were analyzed on line by a gas chromatograph (GAS analyzer XXL1300), NO was analyzed with Xentra 4900C IR analyzer (Servomex). The measurement of NO₂ is done indirectly using a NO₂ to NO converter BÜNOx (Bühler Technologies) by comparison.

The conversion, selectivity and yields of the main products are defined in the following way:

- Conversion: $X_i (\%) = \frac{n_i^{int} - n_i^{out}}{n_i^{int}} * 100$ where n_i^{int} and n_i^{out} are number of mole of the corresponding compounds "i" at the inlet and the outlet of the reactor.
- Selectivity: $S_i (\%) = \frac{x_{in_i}}{\sum_i x_{in_i}} * 100$
- Yield: $Y_i(\%) = X_i * S_i * 100$

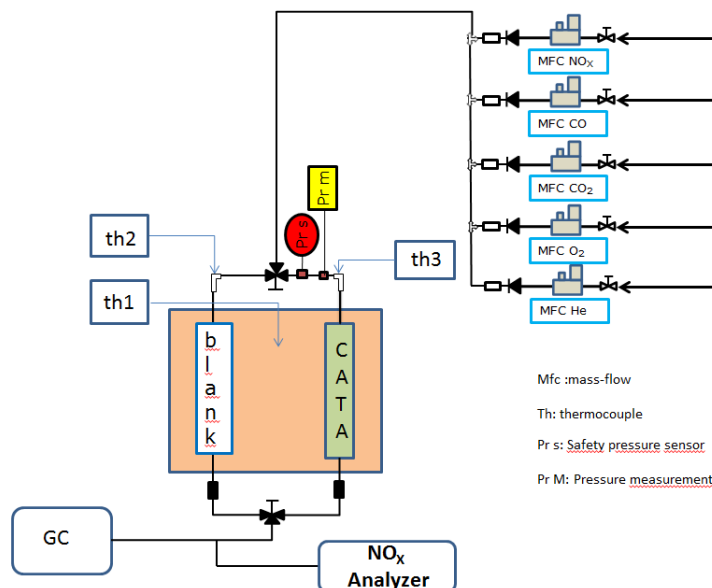


Figure 1: Experimental setup for catalytic purification of CO₂ from oxyfuel combustion

In order to compare the different materials, T_{50} and T_{90} factors will be taken into account. These factors correspond respectively to the temperature at which 50% or 90% of carbon monoxide is converted. For NO reduction, the catalysts will be compared according to their maximum efficiency (yield) at total conversion of CO as the first target is to fully convert CO in CO_2 .

3. Results

The alumina supported catalysts prepared by wet impregnation with precious metal were studied in the catalytic purification of CO_2 . In this work, we studied the effect of nature of metal in this reaction.

3.1. BET surface area

The specific surface area of the alumina and its pore volume were determined by adsorption of nitrogen. Table 2 summarizes the results obtained by the BET and BJH methods.

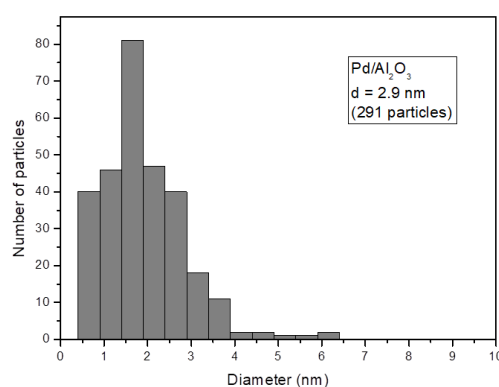
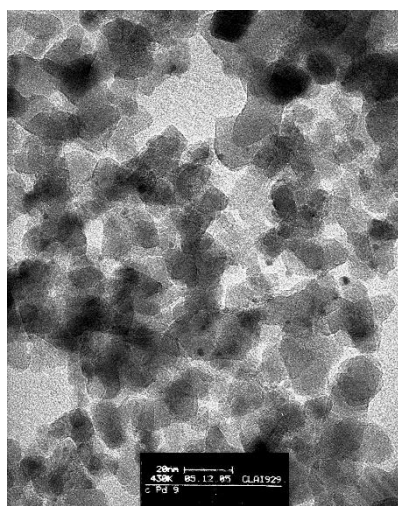
Table 2. Specific surface area and porous volume of alumina

Sample	S_{BET} ($\text{m}^2 \cdot \text{g}^{-1}$)	V_{porous} ($\text{cm}^3 \cdot \text{g}^{-1}$)	Average pore size (nm)
Alumina	100	0.74	31

From these results, the alumina used as support for our catalysts is a mesoporous solid with a large specific surface area.

3.2. TEM and H_2 chemisorption

In order to compare the catalytic activity for our catalysts, we tried to synthesize size-controlled uniform material. We can see in Figure 2 that the synthesized catalytic materials have a quite homogeneous distribution of particle size.



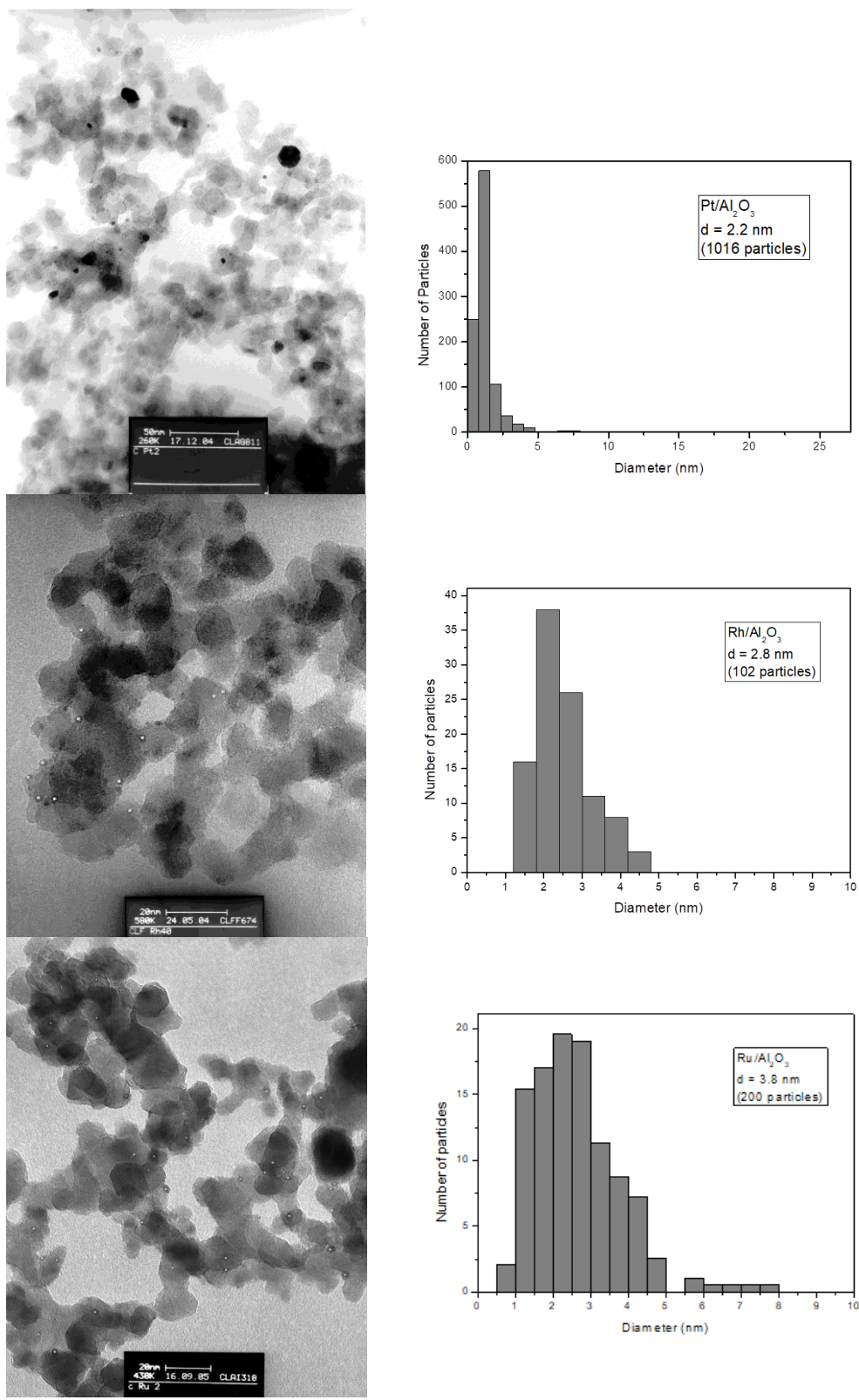


Figure 2. TEM pictures and size distribution of the Al₂O₃ supported Pd, Pt, Rh and Ru catalysts.

Table 3. Properties of catalysts: particles size and metallic accessibility.

Catalysts	Coding	Metallic accessibility (%)	< d > ^a (nm)	< d > ^b (nm)
1% Ir/Al ₂ O ₃	Ir	42	2.2	---

1% Pd/Al ₂ O ₃	Pd	40	2.4	2.9
1% Pt/Al ₂ O ₃	Pt	40	2.3	2.2
1% Rh/Al ₂ O ₃	Rh	41	2.2	2.8
1% Ru/Al ₂ O ₃	Ru	28	3.8	3.8

a Obtained by H₂ chemisorption analysis. b Estimated by TEM pictures.

The results obtained by H₂ chemisorption reported in table 2 evidenced that, Ir, Pd, Pt and Rh on Al₂O₃ catalysts presented a similar and small particle size in a narrow window around 2.3 nm. In the case of Ru/Al₂O₃, the particles were larger than those on the other catalyst samples. These results were in accordance with those obtained by TEM.

3.3. Temperature programmed reduction by H₂

The H₂-TPR measurements were performed to determine the reduction behaviors and oxidation state of various catalysts as depicted in Fig 3. Since the Al₂O₃ support is irreducible from room temperature to 500°C, the peaks of reduction in this temperature range should correspond to the reduction of the different kinds of metallic active phase species.

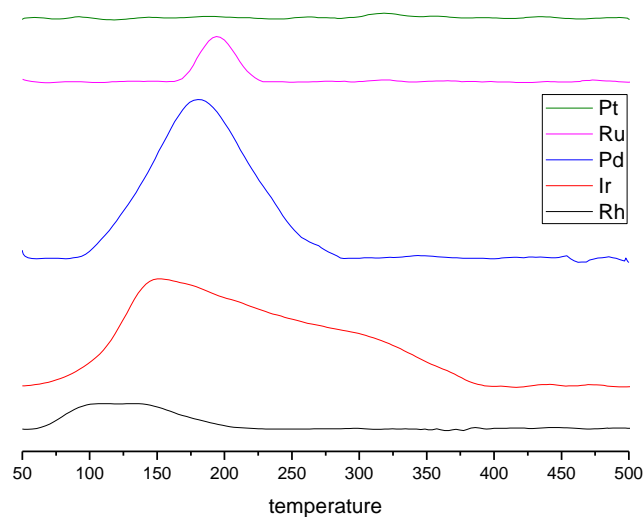


Figure 3. H₂-TPR patterns of the different catalysts (°C)

The TPR profile of Pd supported is characterized by one broad pic centered at around 180°C. According to Ferrer and al. [18] this peak is associated to the reduction of PdOx species that strongly interacts with the support. However, no negative peak was observed at 80°C corresponding to the desorption of hydrogen from PdHx which could be formed at low temperature [16, 19].

The profile of Ru shows a peak with a maximum at about 194°C, which is assigned to Ru oxide reduction already demonstrated by Koopman and al [20].

The Rh profile is composed of a broad reduction peak from ambient to 250°C which is related to the reduction of surface RhO_x species, according to the literature [21–22].

The Ir catalyst exhibits a broad reduction peak between 100-400°C, which can be attributed to the reduction of IrO₂ phase [23,24]. But, usually the reduction IrO₂ phase occurred at higher temperature.

No reduction peak was observed for Pt meaning that Pt nanoparticles should mainly exist in the metallic form (Pt⁰) not accessible for further reduction [23].

As all catalysts were reduced at the end of the preparation and stored under air, some metals can be re-oxidized at room temperature either only in the first layers of the particles surface either until to core oxidation, according to their oxidation resistance and their particles size. Checking metals oxidation state before NO/CO reaction using TPR technique is therefore of great interest. As expected, Pd was deeply re-oxidized as the hydrogen consumption evidenced whereas Rh and Ru were more lightly re-oxidized during the storage. For Ir, the peak temperature observed is lower than usual suggesting that an unstable oxide is formed probably on the first layers of metallic particles. As it concerns platinum, the lack of reduction peak means that the reduction step went to completion during synthesis and that no re-oxidation occurred under air at room temperature or so weakly that the Ar treatment before TPR can remove the oxygen [23].

M. Haneda et al. [25] have shown that NO reduction by CO occurs on stable iridium metal sites. We can therefore assume that the more metallic the species is, the better the activity will be for the reaction studied. Thus, a good platinum activity is expected.

3.4. Catalytic reaction

The catalytic performances of different materials have been studied and determined for the catalytic total CO oxidation and NO reduction with CO in oxidizing atmosphere (10% O₂) and CO₂ rich stream under identical conditions.

Light-off curve of support (Al₂O₃) and NO reduction or oxidation yield have been determined and are reported in fig 4.

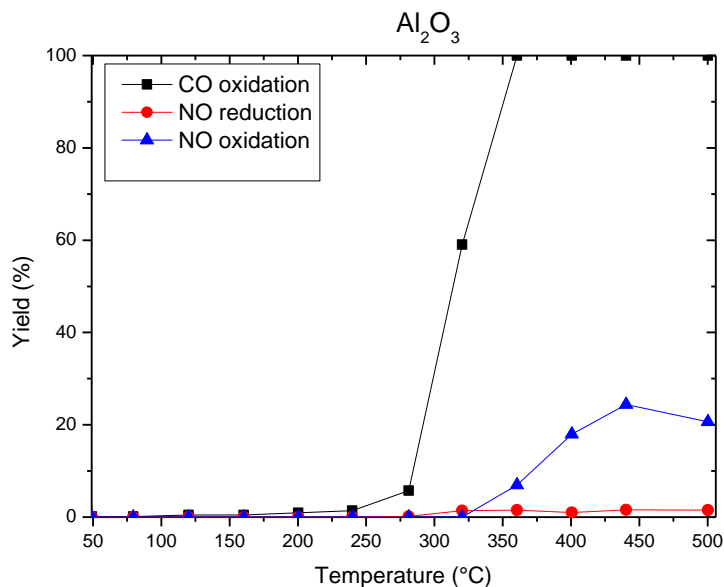


Figure 4. Light-off curves for Al₂O₃ support and NO reduction or oxidation yield

It can thus be seen in fig 4 that on the alumina, it is possible to have a complete oxidation of the CO. For the conversion of NO, there is a slight oxidation of NO at very high temperature but no reduction.

Fig. 5 shows the activities of the catalysts for CO oxidation. They exhibit the activity for this reaction at the temperatures higher than 100°C and the conversion increases with the reaction temperature. For all tests, catalytic performances were compared by considering T₅₀ and T₉₀ for CO oxidation, which respectively correspond to the temperatures at which 50 and 90% of CO were converted. The obtained results are illustrated in Fig. 5. The conversion of CO to CO₂ reached 100% for all studied catalysts. Ir and Rh have a similar activity values with T₅₀ at 236 °C. The general order of catalytic activity, based on the temperature required for 50% conversion (T₅₀) is the following: Pt > Pd > Ir~Rh > Ru.

Considering T₉₀, Pt shows the better performance (176°C), Rh and Ru present a similar activity values with 280°C. The ranking for catalysts does not much change to that obtained at T₅₀: Pt > Pd > Ir > Rh~Ru. The oxidation of CO was investigated on noble metal catalysts supported on TiO₂ by V.P. Santos et al. [26] and they pointed out on metallic particles between 2-4 nm, the same activity order: Pt > Pd > Ir > Rh.

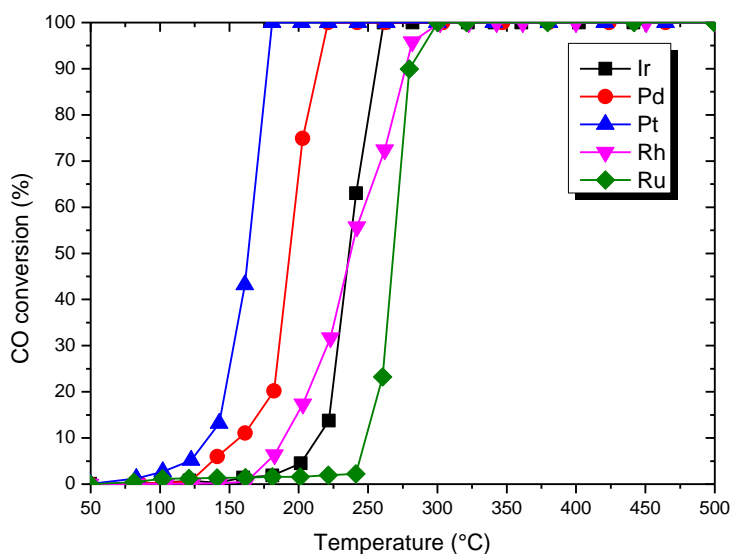
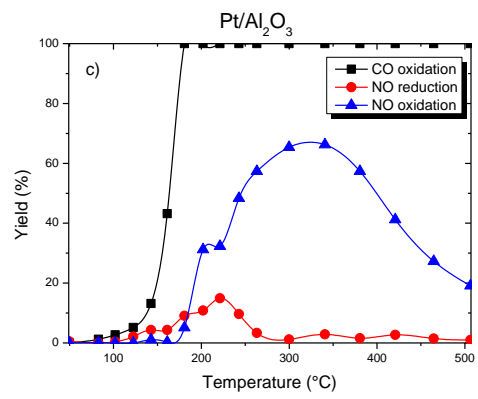
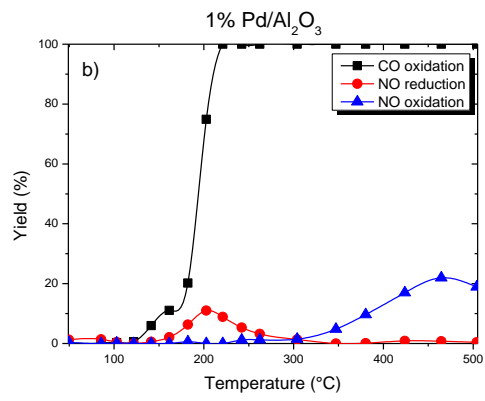
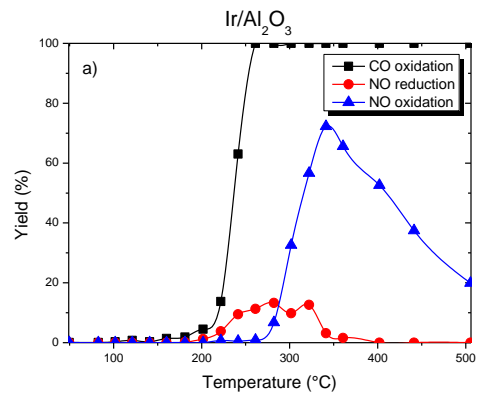


Figure 5. Light-off curves of CO conversion for the different materials. Feedstream composition: 0.02%NO, 0.5% CO, 10% O₂ and 20% CO₂, and balance He. Space velocity: $2.24 \cdot 10^4 \text{ h}^{-1}$

Table 4. T₅₀ and T₉₀ of catalysts catalytic CO oxidation

Catalysts	T ₅₀ (°C)	T ₁₀₀ (°C)
Ir	236	260
Pd	194	212
Pt	164	176
Rh	236	280
Ru	268	280

The oxidation of CO, reduction of NO and oxidation of NO over the impregnated Al₂O₃ with Ir, Pd, Pt, Rh, Ru were evaluated, and the obtained results have been reported in Fig 6.



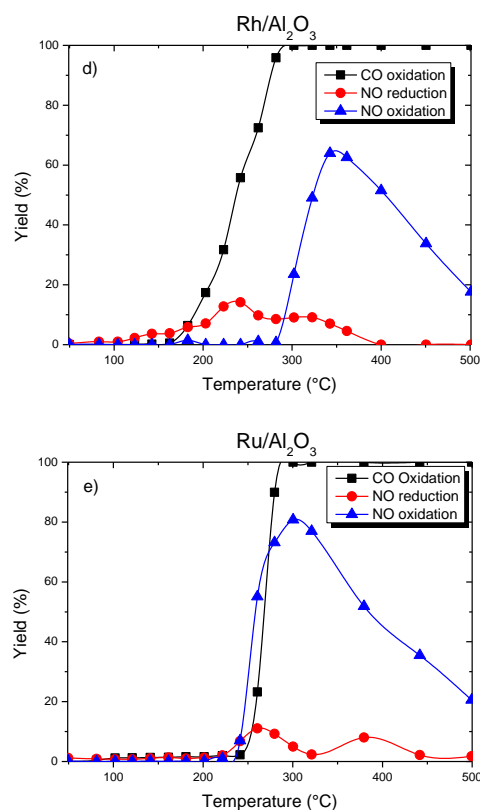


Figure 6. Catalytic activity for the Pt, Rh, Ru, Pd, Ir catalysts supported on alumina. Feedstream composition: 0.02% NO, 0.5% CO, 10% O₂ and 20% CO₂, and balance He. Space velocity: $2.24 \cdot 10^4 \text{ h}^{-1}$

CO is completely oxidized at 260°C with a 13% of NO reduction on Ir/Al₂O₃ (Fig 6-a). The oxidation of NO reaches 72.3% at 340°C.

Pd activity in CO and NO reactions (Fig 6-b) pointed out that the oxidation of CO is carried out at 220°C. NO reduction reaches a maximum with 11% at 200°C.

When using Pt catalyst, CO is totally oxidized at 180°C (Fig 6-c). NO reduction begins from the start of CO oxidation. Pt/Al₂O₃ reduces the NO from 140°C to 300°C with a maximum reduction (14.9%) at 220°C, oxidation phase is also bell-shaped with an optimum (66.2%) at 340°C.

CO oxidation on supported Rh catalyst (Fig 6-d) occurs at higher temperature than with Pt or Pd ones, and the total conversion of CO is only obtained at 300°C. This is in full agreement with the literature on three-way catalysts that use Rh to convert NO_x [12]. With regard to NO conversion, the reduction of NO is 14.4% at 240°C. On the other hand, at 340°C, NO is oxidized at 64.2%.

Similarly to Rh, the total conversion of CO on Ru/Al₂O₃ catalysts (Fig 6-e) is obtained at 300°C and the NO conversion reached 85% including 80% for its oxidation and only 5% for its reduction.

In order to compare and highlight the influence of noble metals nature on the NO reduction with CO in oxidative conditions, the Fig. 7 displays the maxima of NO reduction at total oxidation of CO over all catalysts. The Pt/Al₂O₃ and Ir/Al₂O₃ catalysts exhibit the best performances for NO reduction by CO in presence of an

excess of oxygen and a CO₂ rich stream. Pd, Rh and Ru led to lower activity than Pt and Ir. The yield for NO reduction is similar on these catalysts but at different temperatures: 220°C for Pd, 320 °C for Rh and 380°C for Ru.

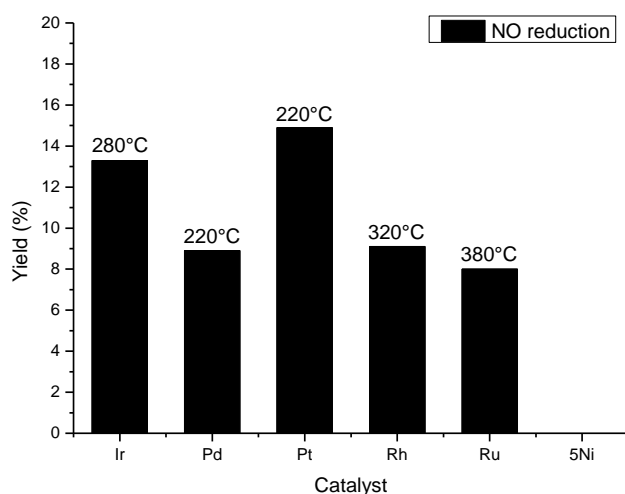


Figure 7. NO reduction at total oxidation of CO. Feedstream composition: 0.02%NO, 0.5% CO, 10% O₂ and 20% CO₂, and balance He. Space velocity: $2.24 \cdot 10^4 \text{ h}^{-1}$

In our results, the low activity of the Pd compare to Ir catalyst could be explain by an oxygen poisoning of the Pd. Almusaiteer and Chuang [27] proved that the presence of O₂ in NO-CO reaction flow plays a role of poison on Pd/Al₂O₃ catalyst. The adsorbed oxygen inhibits N-O dissociation thus causing an accumulation of Pd-N=O and diminution of conversion of NO. On the other hand, Ir has a superior ability than other precious metals to convert NO under oxidizing environment due to its ability to adsorb NO dissociatively in the presence of an excess of O₂ [15]. Tauster and Murell [7] confirmed this result and they proved that Ir is the only catalyst favoring the NO-CO reaction over CO-O₂. The results reported in Fig. 7 evidenced that Ir/Al₂O₃ activity is certainly interesting but Pt/Al₂O₃ exhibits the higher activity for reducing NO by CO in oxidizing environment. Moreover, this interesting performance occurs at a lower temperature than those of the other catalysts. The better performances of Pt and in a lesser extent Ir could be correlated with the TPR results where Pt and Ir were evidenced to be less oxidized than the other catalysts. As expected, the more metallic the species is and remains, the better the activity for NO reduction is despite these oxidizing operating conditions.

4. Conclusion

This work deals with the identification of the best metal catalysts for CO₂ purification in oxidative conditions. In this work, we focus on the NO reduction on alumina supported precious metals using carbon monoxide as reducing agent in oxidizing conditions. First of all, it is possible to achieve the reduction of the NO in an oxidizing medium with a catalytic material by using CO, one of the worst

reducers, but nevertheless always present in the industrial process outputs. The better performances for NO reduction were obtained for Pt/Al₂O₃ catalyst for which the metallic state of particles was evidenced in TPR. The results clearly demonstrated that the more metallic the species is and remains, the better the activity for NO reduction is despite these oxidizing operating conditions. The work is still in progress but it has already proven that NO/CO reaction could be achieved without injection of additional reducers such as ammonia, which can facilitate the implementation of the process and lower the operating cost.

Acknowledgement: This research was funded by: Innocold, Dunkerque LNG, Greater Dunkirk Council and ULCO.

References

1. Olivier, J.G.J., Schure, K.M., Peters, J.A.H.W.; *Trends in global CO₂ and total greenhouse gas emissions: Summary of the 2017 report* - PBL Netherlands Environmental Assessment Agency, - PBL Netherlands Environ. Assess. Agency, **2017**.
2. Dumergues, L.; Favier, B.; Claver, R.A.; *CO₂ Reuse. State of the Art and Expert Opinion Case of waste treatment activities*, **2014**.
3. Iloeje, C.; Field, R.; Ghoniem, A.F.; Modeling and parametric analysis of nitrogen and sulfur oxide removal from oxy-combustion flue gas using a single column absorber, *Fuel*. **2015**, 160, 178–188. doi:10.1016/j.fuel.2015.07.057.
4. Skalska, K.; Miller, J.S.; Ledakowicz, S.; Trends in NO_x abatement : *A review*, **2010**, 408, 3976–3989. doi:10.1016/j.scitotenv.2010.06.001.
5. Malfoy, P. ; *Reduction Catalytique de NO et N₂O par H₂ , CO ou C₃H₈*, **1997**.
6. Hegedus, L.L.; Hertz, R.K.; Oh, S.H.; Aris, R.J.; Effect of Catalyst Reactions Loading on the Simultaneous of NO, CO, and O₂, *J. Catal.* **1979**, 57, 513–515.
7. Tauster, L., Murell, S.J.; The NO-CO Reaction In the Presence of Excess O₂ as Catalyzed by Iridium, *J. Catal.* **1976**, 41, 192–195.
8. Shelef, M.; Otto, K.; Ghandy, H.; The oxidation of CO by O₂ and by NO on supported chromium oxide and other metal oxide catalysts, *J. Catal.* **1968**, 375, 361–375
9. Oh, S.H.; Carpenter, J.E.; Role of NO in inhibiting CO oxidation over alumina-supported rhodium, *J. Catal.* **1986**, 101, 114–122. doi:10.1016/0021-9517(86)90234-4.
10. Voltz, S.E.; Morgan, C.R.; Liederman, D.; Jacob, S.M.; Kinetic study of carbon monoxide and propylene oxidation on platinum catalysts, *Ind. & Eng. Chem. Prod. Res. Dev.* **1973**, 12, 294-301
11. Granger, P.; Parvulescu, V.I.; Catalytic NO_x abatement systems for mobile sources: From three-way to lean burn after-treatment technologies, *Chem. Rev.* **2011**, 111, 3155–3207. doi:10.1021/cr100168g.

12. Barbier, J.; Duprez, D.; Steam Effects in 3-Way Catalysis, *Appl. Catal. B* **1994**, *4*, 105–140.
13. Vedyagin, A.A.; Volodin, A.M.; Stoyanovskii, V.O.; Kenzhin, R.M.; Slavinskaya, E.M.; Mishakov, I.V., Stabilization of active sites in alloyed Pd-Rh catalysts on gamma-Al₂O₃ support, *Catal. Today* **2014**, *238*, 80–86. doi:10.1016/j.cattod.2014.02.056.
14. Kobylinski, T.P.; Taylor, B.W.; The catalytic chemistry of nitric oxide, *J. Catal.* **1974**, *33*, 376–384. doi:10.1016/0021-9517(74)90284-X.
15. Taylor, K.; Schlatter, J.C.; Selective reduction of nitric oxide over noble metals, *J. Catal.* **1980**, *63*, 53–71. doi:10.1016/0021-9517(80)90059-7.
16. Wang, C.-B.; Lee, H.-G.; Yeh, T.-F.; Hsu, S.-N.; Chu, K.-S.; Thermal characterization of titania-modified alumina-supported palladium and catalytic properties for methane combustion, *Thermochim. Acta.* **2003**, *401*, 209–216. doi:10.1016/S0040-6031(02)00567-1.
17. Bond, G.C.; The Origins of Particle Size Effects in Heterogenous Catalysis, *Surf. Sci.* **1985**, *156*, 966–981.
18. Ferrer, V.; Finol, D.; Solano, R.; Moronta, A.; Ramos, M.; Reduction of NO by CO using Pd-CeTb and Pd-CeZr catalysts supported on SiO₂ and La₂O₃-Al₂O₃; *J. Environ. Sci. (China)* **2015**, *27*, 87–96. doi:10.1016/j.jes.2014.05.046.
19. Hosseini, M. ; Etude de catalyseurs Pd / Au déposés sur oxydes poreux, TiO₂ et Composés Organiques Volatils (COV), **2008**.
20. Koopman, P.G.J.; Kieboom, A.P.G.; Van Bekkum, H.; Characterization of ruthenium catalysts as studied by temperature programmed reduction, *J. Catal.* **1981**, *69*, 172–179. doi:10.1016/0021-9517(81)90139-1
21. Zhao, B.; Ran, R.; Cao, Y.; Wu, X.; Weng, D.; Fan, J.; Insight into the effects of different ageing protocols on Rh/Al₂O₃ catalyst, *Appl. Surf. Sci.* **2014**, *308*, 230–236. doi:10.1016/j.apsusc.2014.04.140..
22. McCabe, R.W.; Usmen, R.K.; Ober, K.; Gandhi, H.S.; The effect of alumina phase-structure on the dispersion of Rhodium/Alumina catalysts, *J. Catal.* **1995**, *151*, 385–393; doi:10.1006/jcat.1995.1041.
23. Goula, M. A.; Charisiou, N. D.; Papageridis, K. N.; Delimitis, A.; Papista, E.; Pachatouridou, E.; Iliopoulou, E.F.; Marnellos, G.; Konsolakis, M.; Yentekakis I.V.; A comparative study of the H₂-assisted selective catalytic reduction of nitric oxide by propene over noble metal (Pt, Pd, Ir)/γ-Al₂O₃ catalysts; *J. Env. Chem. Eng.* **2016**, *4*, Issue 2, 1629-1641; doi.org/10.1016/j.jece.2016.02.025
24. Vicerich, M.A.; Benitez, V. M.; Especel, C.; Epron, F.; Pieck C.L.; Influence of iridium content on the behavior of Pt-Ir/Al₂O₃ and Pt-Ir/TiO₂ catalysts for selective ring opening of naphthenes, *Appl. Catal. A* **2013**, *453*, 167–174; doi.org/10.1016/j.apcata.2012.12.015
25. Haneda, M., Fujitani, T., Hamada, H.; Effect of iridium dispersion on the catalytic activity of Ir/SiO₂ for the selective reduction of NO with CO in the presence of O₂ and SO₂; *J. Molec. Catal. A* **2006**, *256*, 143–148

26. Santos, V.P., Carabineiro, S.A.C., Tavares, P.B., Pereira, M.F.R., Órfão, J.J.M., Figueiredo, J.L.; Oxidation of CO, ethanol and toluene over TiO₂ supported noble metal catalysts; *Appl. Catal. B* **2010**, *99*, 198–205
27. Almusaiter, K.; Chuang, S.S.C.; Isolation of Active Adsorbates for the NO–CO Reaction on Pd/Al₂O₃ by Selective Enhancement and Selective Poisoning, *J. Catal.* **1998**, *170*, 161–170.